



HAL
open science

Some Observations on Testing Conditions of High-Temperature Experiments on Concrete: An Insight from Neutron Tomography

Dorjan Dauti, Alessandro Tengattini, Stefano Dal Pont, Nikolajs Toropovs,
Matthieu Briffaut, Benedikt Weber

► **To cite this version:**

Dorjan Dauti, Alessandro Tengattini, Stefano Dal Pont, Nikolajs Toropovs, Matthieu Briffaut, et al..
Some Observations on Testing Conditions of High-Temperature Experiments on Concrete: An Insight
from Neutron Tomography. *Transport in Porous Media*, 2020, 132, pp.299 - 310. 10.1007/s11242-
020-01392-2 . hal-03251848

HAL Id: hal-03251848

<https://hal.science/hal-03251848>

Submitted on 7 Jun 2021

HAL is a multi-disciplinary open access archive for the deposit and dissemination of scientific research documents, whether they are published or not. The documents may come from teaching and research institutions in France or abroad, or from public or private research centers.

L'archive ouverte pluridisciplinaire **HAL**, est destinée au dépôt et à la diffusion de documents scientifiques de niveau recherche, publiés ou non, émanant des établissements d'enseignement et de recherche français ou étrangers, des laboratoires publics ou privés.



1 Some Observations on Testing Conditions 2 of High-Temperature Experiments on Concrete: An Insight 3 from Neutron Tomography

4 Dorjan Dauti¹ · Alessandro Tengattini^{1,2} · Stefano Dal Pont¹ · Nikolajs Toropovs^{3,4} ·
5 Matthieu Briffaut¹ · Benedikt Weber³

6 Received: 19 September 2019 / Accepted: 18 February 2020
7 © Springer Nature B.V. 2020

8 Abstract

9 This communication explores the influence of boundary effects, embedded sensors and
10 crack opening on high-temperature experiments of concrete as revealed by in situ neutron
11 tomography. The hypotheses routinely taken about these experimental aspects in com-
12 mon practice are hereby reassessed in light of the insight given by noninvasive full-field
13 measurements. Notably, we directly assess the heat and moisture insulation techniques and
14 reveal the influence of temperature and gas pressure monitoring on the testing conditions,
15 opening new perspectives toward their improvement.

16 **Keywords** Concrete · High temperature · Neutron tomography · Boundary effect ·
17 Embedded elements

AQ1

A1 Dorjan Dauti
A2 dorjan.dauti@3sr-grenoble.fr

A3 Alessandro Tengattini
A4 Alessandro.Tengattini@3sr-grenoble.fr

A5 Stefano Dal Pont
A6 stefano.dalpont@3sr-grenoble.fr

A7 Nikolajs Toropovs
A8 Nikolajs.Toropovs@empa.ch

A9 Matthieu Briffaut
A10 matthieu.briffaut@3sr-grenoble.fr

A11 Benedikt Weber
A12 Benedikt.Weber@empa.ch

A13 ¹ CNRS, Grenoble INP, 3SR, Université Grenoble Alpes, 38000 Grenoble, France

A14 ² Institut Laue-Langevin, 71 Avenue des Martyrs, 38000 Grenoble, France

A15 ³ Empa, Swiss Federal Laboratories for Materials Science and Technology, Überlandstrasse 129,
A16 8600 Dübendorf, Switzerland

A17 ⁴ Institute of Materials and Structures, Riga Technical University, 1 Kalku Street, Riga 1658, Latvia

18 1 Introduction

19 High-temperature behavior of concrete is an important issue for the structural safety of high-
20 rise buildings, tunnels, nuclear power plants, etc. When these structures are exposed to fire,
21 a phenomenon known as spalling may occur, which consists in the detachment of pieces of
22 concrete from the heated surface. This phenomenon can lead to the premature failure of con-
23 crete structures. For better understanding the physics behind spalling, which is a rather com-
24 plex phenomenon due to the coupled thermo-hydro-mechanical behavior of heated concrete,
25 many laboratory tests have been performed and are documented in the literature. Besides
26 tests on full-scale concrete elements with typical size 3 m (Richter 2004; Boström and Rob-
27 ert 2008), tests on medium-scale specimens with a typical heated surface of 1 m² (Dal Pont
28 and Ehrlacher 2004; Carre et al. 2013; Pereira et al. 2011; Lo Monte and Felicetti 2017) and
29 small-scale specimens (e.g., rectangular prisms or cylinders with edges or diameter/height less
30 than 300 mm) (Kalifa et al. 2000; Dal Pont et al. 2005; Hertz and Sørensen 2005; Van der
31 Heijden et al. 2012; Felicetti and Lo Monte 2013; Tanibe et al. 2014; Toropovs et al. 2015;
32 Lo Monte et al. 2017) have been carried out. In most of these studies, the experimental proce-
33 dure involves embedded elements such as thermocouples and pressure gauges inside concrete
34 specimens to monitor the temperature and gas pressure field. In medium- and small-size tests,
35 which represent only a part of a structural element, some form of heat and moisture insulation
36 is normally applied on the lateral sides of the samples aiming to achieve a uni-dimensional
37 heat and moisture flow. For the moisture insulation, different approaches are routinely used.
38 Self-adhesive aluminum foil was used in Toropovs et al. (2015). Felicetti et al. (2017) tried
39 two different sealing systems: (1) carbon fibers placed on a high-temperature silicon layer pre-
40 viously smeared on the concrete surface and (2) aluminum foil placed on the concrete surface
41 after being both smeared with epoxy resin. The second system turned out to be a better insu-
42 lator according to the mass loss results of a 120 °C drying test in a ventilated oven. Also for
43 the heat insulation, different options can be found in the literature. In Kalifa et al. (2000) and
44 Mindeguia et al. (2010), the lateral sides of the prismatic concrete samples were insulated by
45 porous ceramics blocks. Van der Heijden et al. (2012) insulated their sample with mineral
46 wool. Toropovs et al. (2015) used a 20-mm-thick glass foam layer in their neutron radiogra-
47 phy tests of heated concrete. In Felicetti et al. (2017) and Mugume and Horiguchi (2013), the
48 authors covered their samples with ceramic fiber board.

49 In most of the aforementioned experiments, the validity of the boundary conditions is not
50 directly measured. In this communication, observations from in situ neutron tomography
51 experiments are used to assess the underlying hypotheses. Some of the tests were presented in
52 Dauti et al. (2018a), where the focus was the analysis of the evolution of the moisture profiles,
53 their relation to the temperature profiles, and the influence of the aggregate size on both. Here,
54 we instead focus on some artifacts observed during the experiments, namely the influence
55 of boundary conditions and measurement probes, which can help better appreciate the limit
56 of the hypotheses used when interpreting many experimental results in the literature. These
57 observations rely heavily on the fact that 3D information is available from the tomography
58 tests.

59 2 Neutron Tomography Experiments on Heated Concrete

60 In this section, a brief summary of the neutron tomography experiments is reported. More
 61 details can be found in Dauti et al. (2018a). Neutron tests show the evolution of moisture
 62 within the sample and enable thus much more detailed information than medium and large-
 63 scale test. However, neutrons can penetrate concrete only through a few centimeters. This
 64 technique is thus only applicable to small samples. These tests were performed using cylin-
 65 drical specimens with a diameter of 3 cm, which were cast using commercial plastic con-
 66 tainers as mold, alongside with prismatic samples of $40 \times 40 \times 160 \text{ mm}^3$ for mechanical
 67 properties. Mechanical properties were determined according to Swiss standard SIA 262-1
 68 (similar to the European EN 12390-13 standard). In particular, compressive strength meas-
 69 ured at 28 days on 6 samples (halves of initial 3 prisms used to determine flexural strength)
 70 resulted in 104.1 MPa. As the primary objective of the experimental study was to investi-
 71 gate the influence of the aggregate size, two different concrete mixes, with maximum
 72 aggregate size 8 mm and 4 mm (shown in Table 1), were used. The two mixtures, HPC
 73 8 mm and HPC 4 mm, contained alluvial aggregates, like metamorphic rocks, with maxi-
 74 mum diameter of 8 mm and 4 mm, respectively. The aggregate volume fraction for both
 75 mixtures was of 60% (of the total volume). The specimens were equipped with three ther-
 76 mocouples (type K) for temperature measurement at distances 3 mm, 10 mm, and 20 mm
 77 from the heated surface (Fig. 1). The two wires of the thermocouples enter the concrete
 78 radially from two sides and are welded together at the center. The location of the embedded
 79 thermocouples was imposed during concrete casting. In order to end up with a representa-
 80 tive concrete heating surface at the top with a minimal amount of air bubbles, the samples
 81 were cast upside down with respect to the testing conditions. The thermocouples were thus
 82 located toward the bottom during casting. The samples were vibrated on a vibrating table
 83 until no more visible air bubbles appeared at the surface. Then, they were sealed in plastic
 84 bags and stored in 97% relative humidity and 20°C . Neutron tomography measurements
 85 were performed 28 days after casting.

86 Similarly to Toropovs et al. (2015) and Felicetti et al. (2017), the lateral surface of the
 87 sample was covered with self-adhesive aluminum tape, as shown in Fig. 1 (virtually invis-
 88 ible to neutrons because of their very low interaction with aluminum) to prevent the vapor
 89 from escaping and to obtain a 1D movement of moisture within the heated sample. The
 90 aluminum tape used in the tests (3M High Temperature Aluminum Foil Tape 433) has a
 91 working temperature up to 316°C , which is higher than the temperature experienced by
 92 the sample during the test ($\sim 310^\circ\text{C}$).

Table 1 Concrete mixtures (kg/
 m^3)

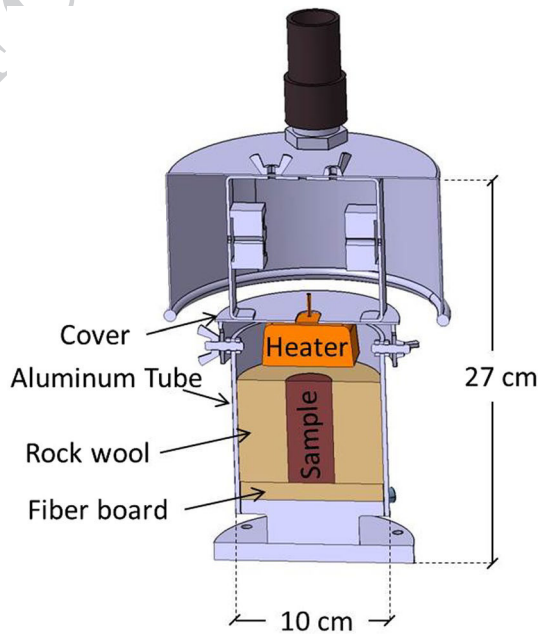
	HPC 4 mm	HPC 8 mm
Cement CEM I 52.5 R	488	488
Silica fume	122	122
Aggregate 0–1 mm	632.8	400
Aggregate 1–4 mm	949.2	600
Aggregate 4–8 mm	0	582
Superplasticizer SIKA 20HE	8.54	8.54
Water	189.1	189.1
w/b total	0.31	0.31

Fig. 1 Specimen equipped with thermocouples and wrapped with adhesive aluminum tape (in testing orientation)



93 The specimen was placed inside a heating cell (Fig. 2). During a test, the specimen was
94 heated on the top face with a ceramic infrared radiator, which reached 500 °C within 3
95 minutes and then was kept at constant temperature. The specimens were surrounded with
96 rockwool, as shown in the drawing in Fig. 2, in order to maximize the uniformity of one-
97 dimensional heating.

Fig. 2 Drawing of the heating cell



98 Neutron tomographies were performed at the NeXT (D50) beamline at the Institut
99 Laue-Langevin (ILL) in Grenoble, France. The principle of neutron tomography is analo-
100 gous to that of X-ray computed tomography. However, in contrast to X-rays, which interact
101 with electrons and whose attenuation thus depends on the atomic number of the atoms they
102 interact with, neutrons interact with the nuclei. The hydrogen atoms of the water molecule
103 highly attenuate neutrons, which makes it possible to detect the evolving moisture con-
104 tent in concrete. In addition, due to the presence of free and chemically bound water, the
105 cement paste has higher neutron attenuation than the aggregates. Thus, the latter can be
106 easily distinguished from the cement matrix. While the sample was being heated, neutron
107 tomographies were performed for measuring in real time the moisture distribution in 3D
108 (Fig. 3). During the heating test, 60 tomographies (3D scans) were taken. Each tomogra-
109 phy, which comprised 500 projections, was acquired in only one minute. Such acquisition
110 time was fast enough for following the rapid dehydration process in concrete.

111 3 Results and Discussion

112 3.1 Boundary Effects

113 One of the challenges when performing experiments on heated concrete is generating a
114 uniform, “1D” heat and moisture flow by adopting the appropriate lateral heat and moisture
115 insulation. Despite the applied insulation for heat and moisture, drying at the boundary
116 was observed in all the tested samples. An example of such a phenomenon is shown in the
117 vertical cut of the 3D volume of sample HPC 8 mm given in Fig. 4. Due to the difference
118 in neutron attenuation between the hydrated and dehydrated cement paste, the drying front
119 is evident in the image. It is clear that the front is not uniform and the precautions taken for
120 obtaining a 1D drying front (rockwool and/or aluminum tape) are insufficient.

121 A hypothetical explanation to this phenomenon could be the fact that because the speci-
122 mens are cast, a “wall effect” appears, meaning cement paste concentration near the mold.
123 However, this hypothesis is not supported by the observations in Dauti et al. (2018a),

Fig. 3 Setup in the NeXT (D50) beamline at Institut Laue-Langevin (ILL)

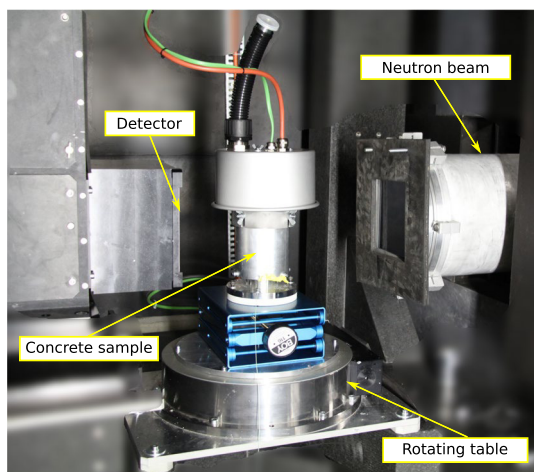
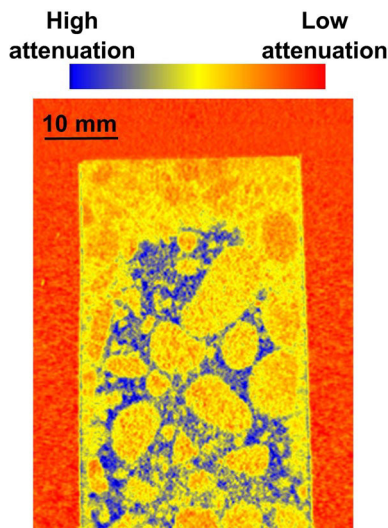


Fig. 4 Vertical cut of the 3D volume, captured at min 48 of heating, highlighting the additional lateral drying



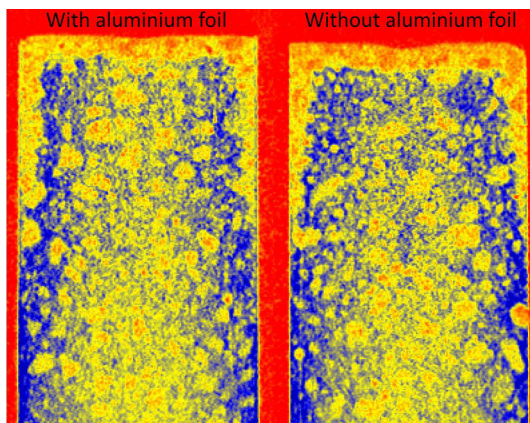
124 where the boundary effect is virtually identical regardless of the aggregate size (4–8 mm
125 maximum diameter).

126 For investigating further the effect of the self-adhesive aluminum foil, two concrete
127 samples HPC 4 mm, with and without aluminum foil, were tested. As shown in Fig. 5, the
128 same boundary effect is observed in both samples. This shows that the influence of the alu-
129 minum tape is minimal.

130 It is worth noting that, in the previous studies, such boundary effect was either assumed
131 negligible in the analysis (Kalifa et al. 2000; Felicetti et al. 2017; Van der Heijden et al.
132 2011), or if it was detected, the 2D nature of the tests made it not quantifiable (Toropovs
133 et al. 2015). The 3D measurements of moisture content by neutron tomography permit the
134 observation and quantification of this boundary effect

135 The direct observation of the boundary effect opens new perspectives for investigat-
136 ing and eventually improving the current experimental practice on lateral insulation for
137 achieving a uni-dimensional drying front. Realistic boundary conditions are not only

Fig. 5 Boundary effect in two samples, with and without aluminum foil



138 important for reproducing as closely as possible the actual conditions of a concrete
139 element submitted to fire, but it is also critical in quantifying important physical phe-
140 nomena such as moisture accumulation. The aspects of the interaction of the bound-
141 ary effect with the quantification of the moisture accumulation are discussed in the
142 following.

143 In a situation where the drying front is not uniform, 3D measurements of moisture
144 content by neutron tomography become even more relevant, and 1D or 2D measure-
145 ments (i.e., neutron radiography, NMR, ground penetrating radar) have to be used with
146 precaution. For instance, in neutron radiography, the recorded intensity is related to the
147 neutron attenuation through the thickness of the sample parallel to the neutron beam.
148 A radiography is a projection resulting from the integration of the signal attenuation in
149 the direction of the beam. The 1D profile is then evaluated by averaging the projection
150 perpendicular to the beam (see Toropovs et al. 2015). The boundary effects perpen-
151 dicular to the neutron beam can be eliminated by considering only an interior region
152 of the radiography. The boundary effect in the beam direction, however, is inherently
153 inextricable in the radiography. This can give misleading results.

154 As an example, the averaging process as obtained from radiography is compared to
155 the averaging obtained from tomography in Fig. 6. The two processes correspond to
156 two different regions:

- 157 • The first region is a disk which excludes the boundaries and represents a region
158 where the front is uniform.
- 159 • The second region is a slice in which we exclude the boundaries only in one direc-
160 tion. Such a region would be representative of the one-dimensional moisture pro-
161 files usually obtained from neutron radiography experiments.

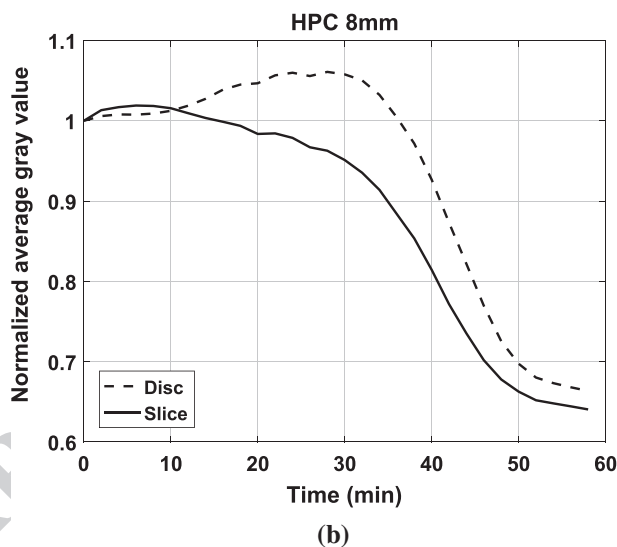
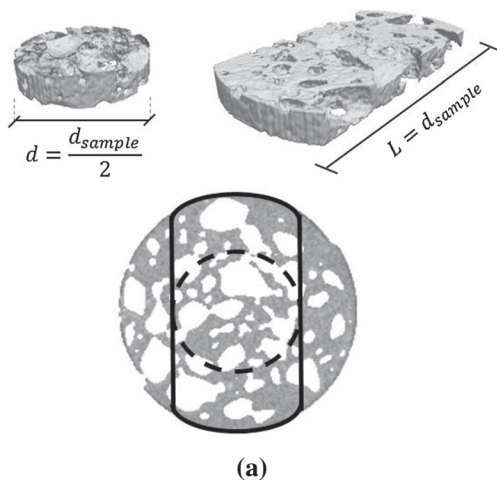
162 The thickness of the disk is of 20 pixels, i.e., 4 millimeters. The purpose of a “thick”
163 disk is merely to reduce statistical noise induced by the high speed of the acquisitions.
164 As such, thinner disk is more noisy but also more spatially detailed.

165 In Fig. 6, the evolution of the average gray value with time for the two regions is
166 compared. Note that what is perceived as gray value in the images is actually directly
167 related to the water content: a high gray value means a high water content. The “gray”
168 images in Figs. 4 and 5 are transformed to color composite images, where blue color
169 means high gray value (high water content). In Fig. 6 the results of the average gray
170 value are normalized to the initial gray value.

171 A clear difference between the two can be observed. In the disk, an increase in the
172 gray value is seen, while the gray value in the slice doesn’t exhibit such an increase
173 due to the boundary effect, which still exists in one direction. An increase in the core is
174 in fact hidden by a decrease near the boundary. This simple example highlights another
175 aspect of the importance of 3D measurements.

176 While the example above demonstrates how the boundary effect can cause an under-
177 estimation of the moisture accumulation, it was shown in a previous study (Dauti
178 et al. 2018a) that the boundary effect can also cause an overestimation of the moisture
179 accumulation when a neutron imaging artifact such as beam hardening takes place.
180 A simplified model for estimating the influence of beam hardening showed that this
181 artifact, together with lateral drying, makes the moisture accumulation appear more
182 pronounced than it actually is.

Fig. 6 Moisture profiles for two regions: a disk (representing the analysis performed in the current study using the neutron tomography results) and a slice (representing the analysis usually performed using neutron radiography results), both represented schematically in (a). The results given in (b) show how the 1D profiles obtained from neutron radiography (solid line) can be misleading due to the boundary effect which is not visible in the direction of the beam



183 3.2 Thermocouple-Induced Air Bubbles

184 Embedded elements (e.g., thermocouples, pressure sensors) are routinely employed in
 185 experiments for measuring parameters such as temperature or pressure in heated con-
 186 crete, which are useful for understanding the behavior of concrete at high temperature.
 187 Nevertheless, the presence of such elements inside concrete might perturb the sample
 188 and affect the measurement. For instance, in Dal Pont (2004), it is postulated that a
 189 cavity, possibly formed around the head of the pressure gauge, has an influence on the
 190 pressure measurement. Similarly, in Jansson (2008), it is claimed that a cavity might
 191 be formed around a thermocouple, resulting in a plateau in the temperature develop-
 192 ment around 100 °C, which is an experimental anomaly often observed because of the
 193 fact that the cavity becomes water-filled and the thermocouple measures the temperature
 194 inside the cavity.

195 Unlike in the aforementioned works, where possible defects are hypothesized, in the
196 reported neutron experiments this alteration of the samples induced by the presence of
197 thermocouples was observed directly, for the first time. Figure 7 shows a horizontal slice at
198 the position of the thermocouple located 20 mm from the heated surface of a sample with
199 HPC 4 mm concrete mix. Air voids are observed around the thermocouple wire which has
200 a diameter of only 0.25 mm. It appears that these air bubbles rose during casting when
201 vibrating and were trapped in the proximity of the wires.

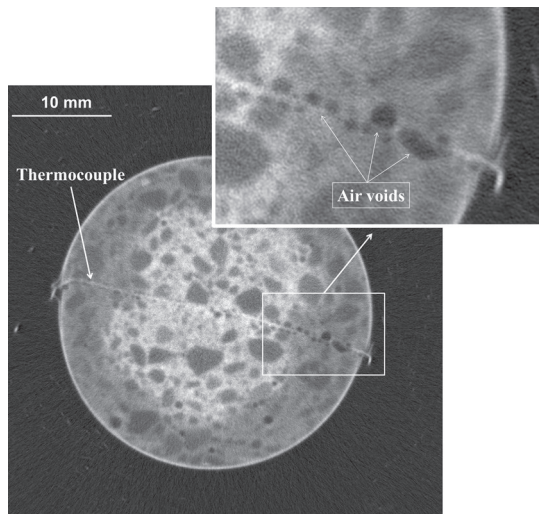
202 This is an important observation for the experimental community on heated concrete,
203 which indicates that even very thin embedded elements such as a thermocouple can be
204 intrusive and can affect locally the material properties and eventually the measurement that
205 is being performed. Such an artifact can become even more substantial when considering
206 other embedded measurement elements such as pressure sensors, the size of which can
207 range from 2 to 12 mm (Jansson 2013). Similarly to what is observed for the thermocou-
208 ples in Fig. 7, air voids around a pressure sensor could build an escape channel for vapor
209 and potentially affect the pressure measurements, which have been extensively used in lit-
210 erature for validating numerical models. While several hypotheses have been postulated
211 in the literature on the disturbance caused by an embedded element (Jansson 2008, 2013;
212 Mugume and Horiguchi 2011), neutron imaging represents an effective method for having
213 a closer look to such perturbations in order to improve the measurement procedures.

214 Using neutron imaging, it is also possible to accurately determine the exact position of a
215 thermocouple. This useful information becomes particularly relevant when considering the
216 validation of numerical models, as even a small change in the position causes a significant
217 difference in the temperature results as shown in Dauti et al. (2018b).

218 3.3 Influence of a Crack on the Drying Front

219 The concrete samples employed in heating tests may contain preexisting cracks due to a
220 number of reasons including shrinkage, disturbance by the embedded elements, demold-
221 ing, etc. In addition, cracks may form during heating (high temperature gradients, thermal
222 incompatibility aggregate–cement paste, etc). These cracks often go unnoticed since they

Fig. 7 Air voids around a thermocouple in a high-resolution image



223 are too small to be detected by the naked eye or are located inside the sample. In this sec-
224 tion, the detection and the influence that a crack can have on the drying front are discussed.

225 A heating test in which a crack has been observed to influence the drying front is pre-
226 sented in the following. Note that the experimental procedure followed for this test is the
227 same as the one described in Sect. 2. The sample (HPC 4 mm) was equipped with thermo-
228 couples and no crack was observable when looking at the sample with naked eye before the
229 test. Vertical slices of the tomographies, obtained at different times, are shown in Fig. 8. A
230 diagonal crack, initiated at the position of the thermocouple, possibly due to the voids sur-
231 rounding it, created a diagonal drying path alongside it. The reason may be related to the
232 physical process of dehydration occurring predominantly around a crack, where vapor can
233 escape and the pore pressure is low.

234 4 Conclusion

235 Neutron tomography experiments on concrete have revealed important information related
236 to the commonplace experimental procedures employed in the study of the behavior of
237 concrete at high temperature with respect to spalling.

238 It has been observed that the heat and moisture insulation techniques that have been
239 adopted in this study, as well as in other studies in the literature, are not sufficient, as all the
240 tested samples experience some degree of lateral drying. This yields a non-uniform drying
241 front, which not only affects the representativity of the sample with respect to a concrete
242 element subjected to fire, but is also critical in quantifying important physical phenomena
243 such as moisture accumulation.

244 Tomography images have shown that air voids can form around thermocouples result-
245 ing in a perturbation of the monitored parameters. Such an observation is important for the
246 experimental community, not only in the case of a thermocouple, but also when employing
247 other embedded elements, such as a pressure gauge, as the validation of many state-of-the-
248 art models on heated concrete are based on the pressure measurements.

249 The 3D information from tomography also gives insight into the influence that a crack,
250 which is not visible with naked eye, can have on the drying front.

251 It is important to emphasize that the observations presented in this study are based on
252 small-scale experiments ($d = 3$ cm). Such kinds of experiments are crucial for understand-
253 ing the physical phenomena involved in fire spalling of concrete. In addition, they provide

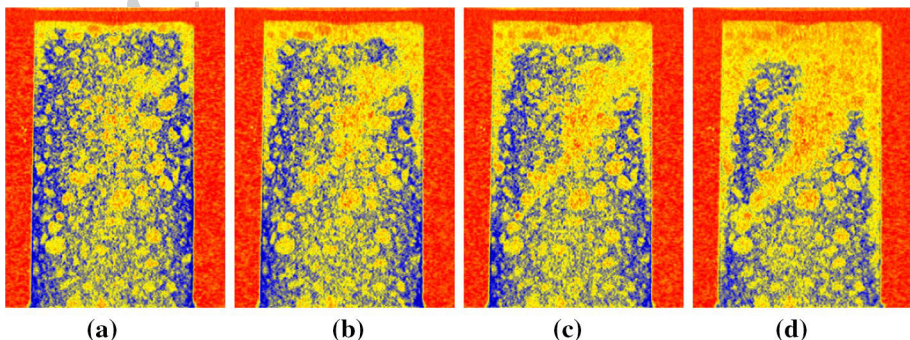


Fig. 8 Vertical cut at **a** 20 min, **b** 26 min, **c** 30 min and **d** 42 min

254 important data for validating the numerical models for predicting spalling. Therefore, the
255 authors believe that the findings presented hereby reveal important information for the
256 experimental community on concrete at high temperature and can be employed in the per-
257 spective of improving the experimental procedures.

258 **Acknowledgements** This study was partially financed by LabEx TEC21 (Investissements d'Avenir-Grant
259 Agreement No. ANR-11-LABX-0030). The authors gratefully acknowledge Université Grenoble Alpes and
260 Empa Laboratories for supporting this experimental campaign.

261 References

- 262 Boström, L., Robert, J.: Report in SP technical research Institute of Sweden (2008)
- 263 Carre, H., Pimienta, P., La Borderie, C., Pereira, F., Mindeguia, J.C.: In: MATEC Web of Conferences, vol.
264 6, p. 01007 (2013). <https://doi.org/10.1051/mateconf/20130601007>
- 265 Dal Pont, S.: Lien entre la perméabilité et l'endommagement dans les bétons à haute température. Ph.D.
266 thesis, ENPC (2004)
- 267 Dal Pont, S., Ehrlicher, A.: Numerical and experimental analysis of chemical dehydration, heat and mass **AQ2**
268 transfers in a concrete hollow cylinder submitted to high temperatures. *Int. J. Heat Mass Transf.* **47**(1),
269 135 (2004). [https://doi.org/10.1016/S0017-9310\(03\)00381-8](https://doi.org/10.1016/S0017-9310(03)00381-8)
- 270 Dal Pont, S., Colina, H., Dupas, A., Ehrlicher, A.: An experimental relationship between complete liquid
271 saturation and violent damage in concrete submitted to high temperature. *Mag. Concrete Res.* **57**(8),
272 455 (2005). <https://doi.org/10.1680/macr.2005.57.8.455>
- 273 Dauti, D., Tengattini, A., Dal Pont, S., Toropovs, N., Briffaut, M., Weber, B.: Analysis of moisture migration
274 in concrete at high temperature through in-situ neutron tomography. *Cem. Concrete Res.* **111**, 41
275 (2018a). <https://doi.org/10.1016/j.cemconres.2018.06.010>
- 276 Dauti, D., Dal Pont, S., Weber, B., Briffaut, M., Toropovs, N., Wyrzykowski, M., Sciumé, G.: Modeling
277 concrete exposed to high temperature: impact of dehydration and retention curves on moisture migration.
278 *Int. J. Numer. Anal. Methods Geomech.* **42**(13), 1516 (2018b)
- 279 Felicetti, R., Lo Monte, F.: In: MATEC Web of Conferences, vol. 6, p. 03001 (2013). <https://doi.org/10.1051/mateconf/20130603001>
- 280 Felicetti, R., Lo Monte, F., Pimienta, P.: A new test method to study the influence of pore pressure on fracture
281 behaviour of concrete during heating. *Cem. Concrete Res.* **94**, 13 (2017). <https://doi.org/10.1016/j.cemconres.2017.01.002>
- 282 Hertz, K., Sørensen, L.: Test method for spalling of fire exposed concrete. *Fire Saf. J.* **40**(5), 466 (2005).
283 <https://doi.org/10.1016/j.firesaf.2005.04.001>
- 284 Jansson, R.: Material properties related to fire spalling of concrete. Licentiate thesis, Division of Building
285 Materials (2008)
- 286 Jansson, R.: Fire spalling of concrete: theoretical and experimental studies. Ph.D. thesis, KTH, Concrete
287 Structures (2013)
- 288 Kalifa, P., Menneteau, F.D., Quenard, D.: Spalling and pore pressure in HPC at high temperatures. *Cem.*
289 *Concrete Res.* **30**(12), 1915 (2000). [https://doi.org/10.1016/S0008-8846\(00\)00384-7](https://doi.org/10.1016/S0008-8846(00)00384-7)
- 290 Lo Monte, F., Felicetti, R.: Heated slabs under biaxial compressive loading: a test set-up for the assess-
291 ment of concrete sensitivity to spalling. *Mater. Struct.* **50**(4), 192 (2017). <https://doi.org/10.1617/s11527-017-1055-1>
- 292 Lo Monte, F., Lombardi, F., Felicetti, R., Lualdi, M.: Ground-penetrating radar monitoring of concrete
293 at high temperature. *Constr. Build. Mater.* **151**, 881 (2017). <https://doi.org/10.1016/j.conbuildmat.2017.06.114>
- 294 Mindeguia, J.C., Pimienta, P., Noumow, A., Kanema, M.: Temperature, pore pressure and mass variation of
295 concrete subjected to high temperature: experimental and numerical discussion on spalling risk. *Cem.*
296 *Concrete Res.* **40**(3), 477 (2010). <https://doi.org/10.1016/j.cemconres.2009.10.011>
- 297 Mugume, R.B., Horiguchi, T.: In: 2nd International RILEM Workshop on Concrete Spalling due to Fire
298 Exposure, pp. 87–94 (2011)
- 299 Mugume, R., Horiguchi, T.: In: MATEC Web of Conferences, vol. 6, p. 03002 (2013). <https://doi.org/10.1051/mateconf/20130603002>
- 300 Pereira, F., Pistol, K., Korzen, M., Weise, F., Pimienta, P., Carré, H., Huismann, S.: In: 2nd International
301 RILEM Workshop on Concrete Spalling due to Fire Exposure, pp. 369–377 (2011)

- 307 Richter, E.: Fire Design of Concrete Structures: What Now? What Next?, pp. 261–268. Brescia, Starrylink **AQ3**
308 (2004)
- 309 Tanibe, T., Ozawa, M., Kamata, R., Rokugo, K.: Steel ring-based restraint of HSC explosive
310 spalling in high temperature environments. *J. Struct. Fire Eng.* **5**(3), 239 (2014). <https://doi.org/10.1260/2040-2317.5.3.239>
- 311
- 312 Toropovs, N., Lo Monte, F., Wyrzykowski, M., Weber, B., Sahmenko, G., Vontobel, P., Felicetti, R., Lura,
313 P.: Realtime measurements of temperature, pressure and moisture profiles in high-performance con-
314 crete exposed to high temperatures during neutron radiography imaging. *Cem. Concrete Res.* **68**, 166
315 (2015). <https://doi.org/10.1016/j.cemconres.2014.11.003>
- 316 Van der Heijden, G., Huinink, H., Pel, L., Kopinga, K.: One-dimensional scanning of moisture in heated
317 porous building materials with NMR. *J. Magn. Reson.* **208**(2), 235 (2011). <https://doi.org/10.1016/j.jmr.2010.11.010>
- 318
- 319 Van der Heijden, G., Pel, L., Adan, O.: Fire spalling of concrete, as studied by NMR. *Cem. Concrete Res.*
320 **42**(2), 265 (2012). <https://doi.org/10.1016/j.cemconres.2011.09.014>

321 **Publisher's Note** Springer Nature remains neutral with regard to jurisdictional claims in published maps and
322 institutional affiliations.

323

Journal: 11242
Article: 1392

Author Query Form

Please ensure you fill out your response to the queries raised below and return this form along with your corrections

Dear Author

During the process of typesetting your article, the following queries have arisen. Please check your typeset proof carefully against the queries listed below and mark the necessary changes either directly on the proof/online grid or in the 'Author's response' area provided below

Query	Details Required	Author's Response
AQ1	Kindly check and confirm that the corresponding author is correctly identified.	
AQ2	Please check and confirm the inserted article title is correct for references Dal Pont and Ehrlacher (2004), Lo Monte and Felicetti (2017), Kalifa et al. (1915, 2000), Dal Pont et al. (2005), Hertz and Srensen (2005), Van der Heijden et al. (2011, 2012), Tanibe et al. (2014), Toropovs et al. (2015), Lo Monte et al. (2017), Felicetti et al. (2017), Mindeguia et al. (2010), Dauti et al. (2018a, b).	
AQ3	Please check and confirm the inserted publisher name is correct for reference Richter (2004).	